THE JOURNAL OF PHYSICAL CHEMISTRY LETTERS
A JOURNAL OF THE AMERICAN CHEMICAL SOCIETY

pubs.acs.org/JPCL

Letter

X-ray Free Electron Laser-Induced Synthesis of ε-Iron Nitride at High Pressures

Huijeong Hwang, Taehyun Kim, Hyunchae Cynn, Thomas Vogt, Rachel J. Husband, Karen Appel, Carsten Baehtz, Orianna B. Ball, Marzena A. Baron, Richard Briggs, Maxim Bykov, Elena Bykova, Valerio Cerantola, Julien Chantel, Amy L. Coleman, Dana Dattlebaum, Leora E. Dresselhaus-Marais, Jon H. Eggert, Lars Ehm, William J. Evans, Guillaume Fiquet, Mungo Frost, Konstantin Glazyrin, Alexander F. Goncharov, Zsolt Jenei, Jaeyong Kim, Zuzana Konôpková, Jona Mainberger, Mikako Makita, Hauke Marquardt, Emma E. McBride, James D. McHardy, Sébastien Merkel, Guillaume Morard, Earl F. O'Bannon, III, Christoph Otzen, Edward J. Pace, Alexander Pelka, Charles M. Pépin, Jeffrey S. Pigott, Vitali B. Prakapenka, Clemens Prescher, Ronald Redmer, Sergio Speziale, Georg Spiekermann, Cornelius Strohm, Blake T. Sturtevant, Nenad Velisavljevic, Max Wilke, Choong-Shik Yoo, Ulf Zastrau, Hanns-Peter Liermann, Malcolm I. McMahon, R. Stewart McWilliams,* and Yongjae Lee*

Cite This: *J. Phys. Chem. Lett.* 2021, 12, 3246–3252

Read Online

ACCESS | Metrics & More | Article Recommendations

ABSTRACT: The ultrafast synthesis of ε-Fe_3N_{1+x} in a diamond-anvil cell (DAC) from Fe and N_2 under pressure was observed using serial exposures of an X-ray free electron laser (XFEL). When the sample at 5 GPa was irradiated by a pulse train separated by 443 ns, the estimated sample temperature at the delay time was above 1400 K, confirmed by *in situ* transformation of α- to γ-iron. Ultimately, the Fe and N_2 reacted uniformly throughout the beam path to form $Fe_3N_{1.33}$, as deduced from its established equation of state (EOS). We thus demonstrate that the activation energy provided by intense X-ray exposures in an XFEL can be coupled with the source time structure to enable exploration of the time-dependence of reactions under high-pressure conditions.

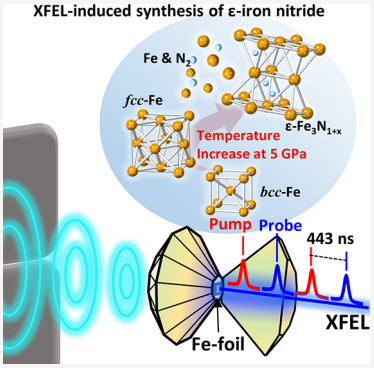

Solid–gas reactions at high pressures and in high radiation environments are important in space and on (exo-) planets.[1] In such environments copious amounts of molecular nitrogen are found together with common refractory materials, such as iron alloys. On Earth, better understanding of the processes guiding the evolution of atmospheric nitrogen on Earth, from its presence in a protoplanetary disc[2] to its present-day appearance in deep mantle reservoirs, is needed.[3,4]

In addition, recent theoretical work on solid–gas reactions such as Mg with Xe, Kr and Ar,[5] iron and nickel with xenon,[6] Kr with oxygen,[7] and the possible formation of helium compounds[8] warrants extensive exploratory synthesis efforts. The recent synthesis of a NiAr Laves phase[9] and $(Xe,Si)O_2$[10] supports changes of electronegativity at high pressures[11] and the opportunity to synthesize new materials with unusual properties.

High-pressure chemical synthesis is important because it permits the exploration of novel compounds at extreme conditions encountered in Earth and space science.[12] Diamond-anvil cell (DAC) experiments are suitable for such studies because the contained gas can function simultaneously as a pressure-transmitting medium (PTM) and a reactant. To trigger a chemical reaction, the energy of intense electromagnetic radiation pulses can be used.[13] Time-resolved diffraction and spectroscopic studies in a DAC at XFEL facilities have the potential to elucidate the formation and dynamics of new materials under extreme conditions.

Here we present an experimental setup using a DAC containing an Fe foil and N_2 as a PTM and reactant to

Received: January 14, 2021
Accepted: March 13, 2021
Published: March 25, 2021

https://doi.org/10.1021/acs.jpclett.1c00150
J. Phys. Chem. Lett. 2021, 12, 3246–3252

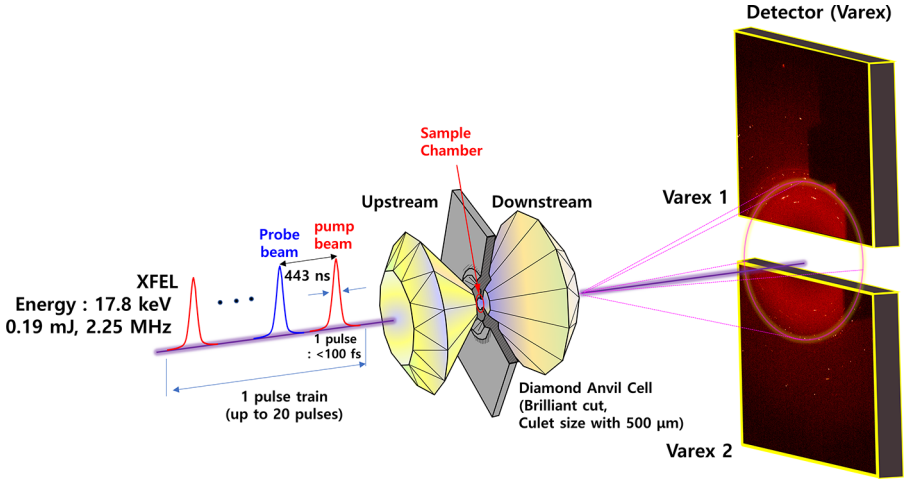

Figure 1. Experimental setup of the XFEL pump-and-probe using the DAC. Schematic diagram of the experimental setup at HED (High Energy Density science) Beamline at European XFEL.

Table 1. Pump and Probe Conditions Used in Our Experiment

Experimental run	XFEL pump and probe condition	
A	2.25 MHz, 0.19 mJ/pulse, 17.8 keV, XFEL beam diameter: 14 μm ⌀	With increasing XFEL transmission from 10% to 100% (2 pulses per train)
B		20 consecutive pulses at 100% transmission (20 pulses in one train)
C		2 consecutive pulses per train at 100% transmission for 11 s (220 exposures)

demonstrate that a reaction to form ε-Fe_3N_{1+x} can be induced by appropriate XFEL pulse-probe conditions.

In addition to cosmochemical and planetary aspects,[14] iron nitrides have important technological applications due to their greater magnetization compared to iron oxides and lower manufacturing cost compared to iron alloys.[15,16] In general, iron nitrides are synthesized by reacting Fe and NH_3 above 400 °C where Fe catalyzes the decomposition of ammonia. Atomic nitrogen then diffuses into bulk Fe with reaction times in the order of 100 s to form a nitride surface layer.[17] Our experiments here show that we can synthesize uniform ε-Fe_3N_{1+x} within nanoseconds without using conventional heating at an initial pressure of 5 GPa within a DAC. Previously, Hasegawa and Yagi synthesized Fe_2N using a laser-heated DAC at pressures up to 10 GPa and temperatures near 1800 ± 50 K.[18] Additional high-pressure and high-temperature syntheses of iron nitrides have led to the discovery of new Fe−N compounds such as α''-$Fe_{16}N_2$, α'-Fe_8N, γ'-Fe_4N, ε-Fe_3N_{1+x} ($-0.40 < x < 0.48$), Fe_7N_3, ζ-Fe_2N, γ'''-FeN, and most recently, Fe_3N_2, FeN_2, and FeN_4.[18−24] On the other hand, Laniel *et al.* revealed that after decompression of a laser-heated DAC to 5 GPa only Fe_2N was found, while above 17.7 GPa NiAs-type FeN was the most stable phase found after pressure release.[23] No indications for the presence of ε-Fe_3N_{1+x} was found in these studies up to pressures of 128 GPa. However, work by Clark *et al.* using ^{57}Fe−Mössbauer studies revealed a mixture of ζ-Fe_2N and ε-Fe_3N_{1+x} after laser heating at 1300 K below 10 GPa.[19]

Our experiments were performed at the High Energy Density (HED) instrument at the European X-ray Free Electron Laser (EuXFEL) facility in Schenefeld, Germany.[25−28] Pulses of 20 fs duration at 17.8 keV were generated in a train of 2−20 pulses at a 2.25 MHz repetition rate, repeating at 10 Hz. The fluence incident on the DAC at 100% transmission was 187(48) μJ/pulse over a spot size of 14 ± 1 μm fwhm, focused by the compound refractive lens (CRL), as measured using damage imprinting in freestanding Ta foil. At this repetition rate, XFEL pulses were so close in time (443 ns) that they may be used to pump and probe *in situ* chemical reactions.[13,29]

A DAC with 500 μm culets was used as a precompression chamber. A small piece of a 4 μm thick Fe foil (<250 μm × 250 μm, 99.99% purity) was loaded into a cylindrical chamber of 310 μm diameter and 50 μm height made by electro-spark erosion in a preindented rhenium gasket (Figure 1). A small spherical ruby crystal with ∼10 μm diameter was placed into the sample chamber to determine the pressure.[30,31] We then loaded N_2 gas as a pressure-transmitting medium (PTM) and a reactant

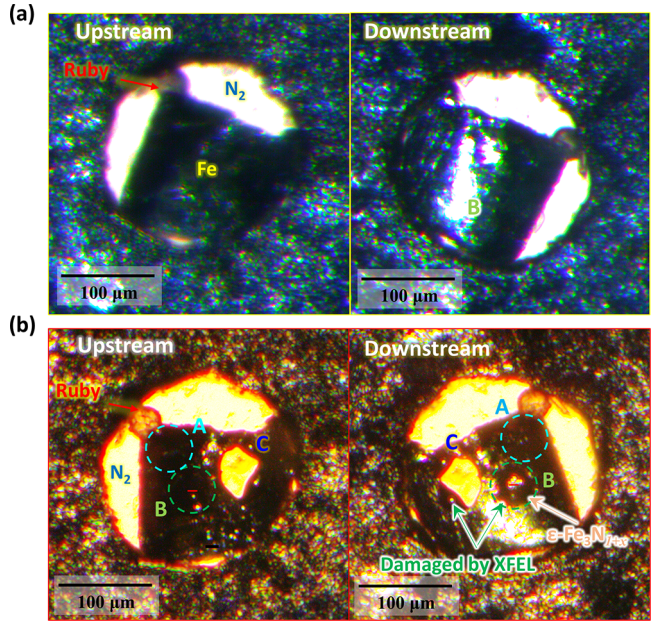

Figure 2. Photos of the sample inside DAC (a) before and (b) after a series of XFEL exposures as described in Table 1. The red line in panel b has been cross-sectioned by FIB for SEM and STEM imaging (see Figure 4).

https://doi.org/10.1021/acs.jpclett.1c00150
J. Phys. Chem. Lett. 2021, 12, 3246−3252

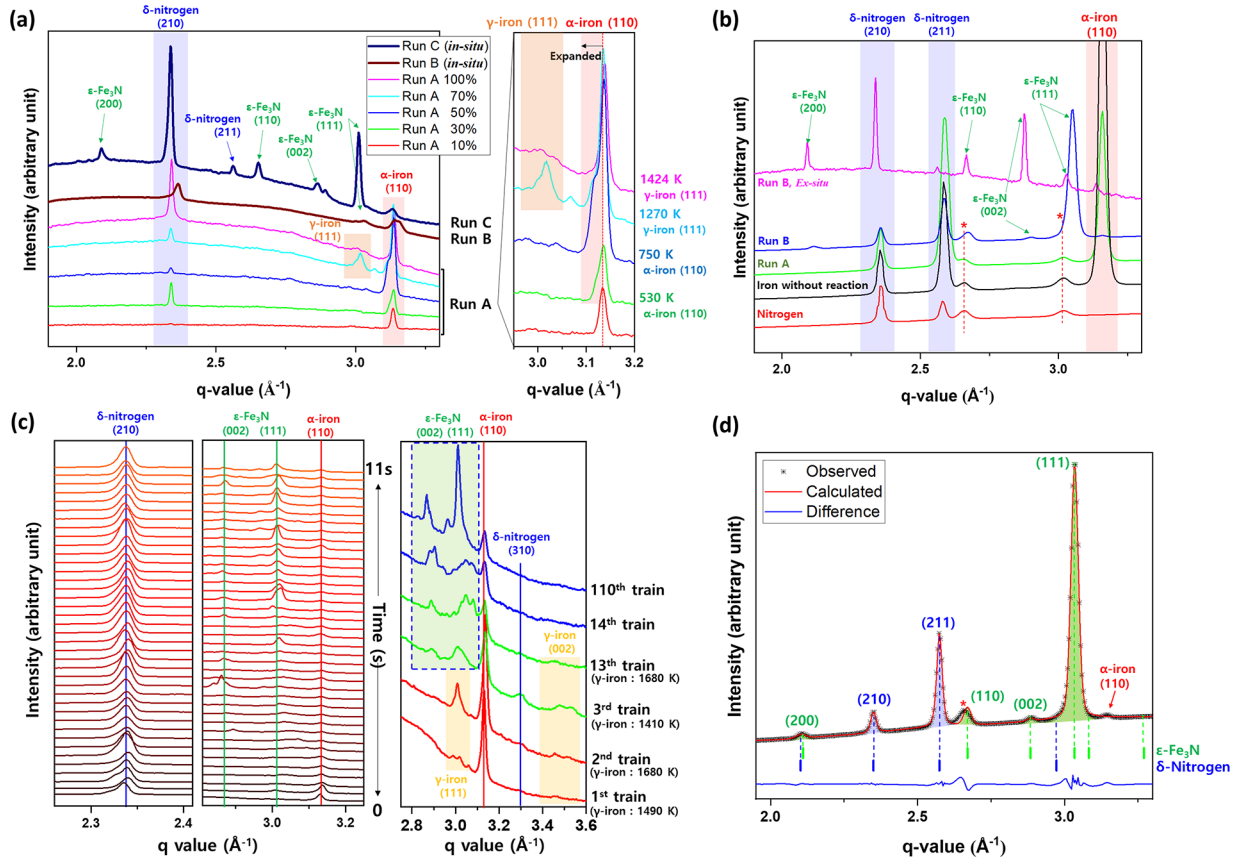

Figure 3. Changes of X-ray diffraction patterns of iron and nitrogen during and after *in situ* chemical reaction by XFEL pump-and-probe. (a) Changes in diffraction patterns of the Fe foil under N_2 PTM precompressed to 5 GPa in a DAC. The percentages in run A indicate the transmission (fluence) of the XFEL. At 100% XFEL transmission, run B contains 20 consecutive pulses while run C has consecutive pulses over 11 s. (b) Synchrotron X-ray diffraction patterns collected at beamline P02.2 at PETRA III after run B, compared to the XFEL data measured right after run B (top pattern). After the XFEL experiments, the sample pressure has changed from 5.0(1) GPa to 7.8(1) GPa. (c) Changes in the diffraction patterns of the Fe foil during run C. (d) Profile fitting of the *ex situ* XRD pattern measured after run B as shown in panel b. ε-Fe_3N_{1+x} ($P6_322$) and δ-Nitrogen ($Pm3n$) were fitted to an agreement index of R_{wp} = 1%. Observed data are shown in black crosses, and the calculated pattern is a red line. Tick-marks under the pattern indicate the (hkl) reflection positions of the composing phases (green, ε-Fe_3N_{1+x}; blue, δ-nitrogen). The red asterisk is an unidentified shoulder peak.

using the gas loading system at the Extreme Conditions Science Infrastructure (ECSI) of PETRA III. The pressure of the sample inside the DAC was determined by recording the shift of the R1 emission line of ruby (precision: ±0.1 GPa). The initial pressure of the sample before XFEL irradiation was set at 5.0(1) GPa. Prior to the experiment, the sample was characterized by synchrotron X-ray diffraction and optical techniques at the Extreme Conditions Beamline, P02.2, at PETRA III to confirm the presence of pure N_2 and Fe in the sample.

The horizontally polarized EuXFEL X-ray beam was directed along the central axis of the DAC, through both diamond culets (Figure 1). Powder X-ray diffraction patterns were collected at 10 Hz using two VAREX XRD4343 area detectors placed above and below the perpendicular direction of the XFEL beam (Figure 1). Patterns comprise a superposition of all scattering during each pulse train, allowing reactions to be tracked in a pump and probe fashion, while repeatedly exposing the sample. We recorded the X-ray diffraction pattern using different combinations of the XFEL fluence and pulses as summarized in Table 1. Dioptas software was used to convert two-dimensional diffraction images to one-dimensional diffraction patterns.[32] Following the *in situ* XFEL measurements, *ex situ* X-ray powder diffraction data of the reaction product were collected at the P02.2 beamline at PETRA III using a monochromatic synchrotron X-ray beam with 0.2898(1) Å wavelength and a PerkinElmer XRD 1621 flat-panel detector. The incident X-ray beam on the sample was focused to 2 μm fwhm beam using a pair of Kirkpatrick Baez (KB) mirrors. The CeO_2 powder standard from NIST SRM 674b was used to calibrate the detector parameters using Dioptas. A 200 μm × 200 μm sample area was grid-scanned in 21 × 21 steps with 1 s exposure time per step.

Figure 2 shows photographic images of the sample before and after the XFEL experiments. Areas irradiated by the three different XFEL pump-and-probe modes are marked with A, B, and C (Table 1). While area A appears to be intact after exposure during run A (increasing pulse fluence), areas B and C visibly show partial and complete alteration of the sample, after 20 consecutive pulses and continuous exposure with 2 consecutive pulses for 11 s, respectively. It should be noted that during exposure runs B and C, *in situ* XRD patterns showed the presence of both the reaction product and compressed solid N_2 (Figure 3c). The observed damage on area C in Figure 2b is interpreted to result from the indirect effects of the X-ray absorption and heating in the sample leading to reaction.

Real-time changes in the X-ray diffraction patterns as a function of XFEL irradiation are summarized in Figure 3. First, we measured the XRD patterns using two consecutive pulses by changing the XFEL fluence to 10%, 30%, 50%, 70%, and 100% (run A) to check the stability of the sample and the diamond

https://doi.org/10.1021/acs.jpclett.1c00150
J. Phys. Chem. Lett. 2021, 12, 3246−3252

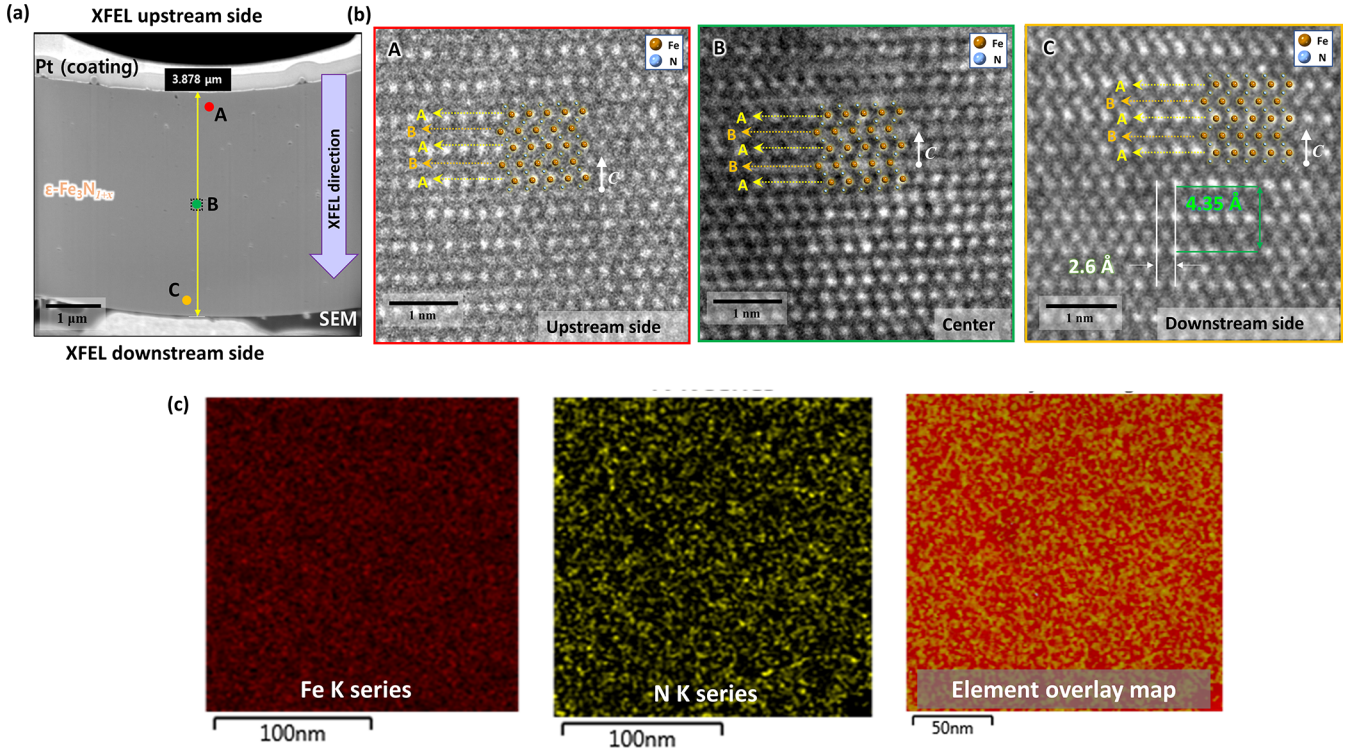

Figure 4. Electron microscopy images and elemental mapping of the recovered sample. (a) Cross-sectional SEM image after exposure run B (the red line in Figure 2b). (b) The positions of the red, orange, and green area in the SEM image are shown by the STEM images. (c) Energy dispersive spectroscopy (EDS) elemental mapping of iron (left), nitrogen (middle), and their overlay (right) at the middle of the recovered sample (the green area in the SEM image).

anvil cell. In each two-pulse exposure, the first pulse probed the sample at ambient temperature and also increased its temperature as a result of the X-ray absorption. The second X-ray pulse probed the sample 443 ns after the first, measuring diffraction peaks that are shifted to lower q values, where the relative shift was used to estimate the temperature at this time (530−1424 K). The peak sample temperature was higher because of cooling between exposures, ranging from 700 to 5700 K in the Fe for 10−100% transmitted power.[29]

As the XFEL fluence increased from 10 to 100% transmission (~10^{10} to ~10^{11} photons per pulse), the diffraction peak intensities of the compressed solid N_2 and bcc-Fe (α-iron) increase as expected, which demonstrates that the anvils remain intact and maintain the original compression conditions (Figure 3a). At 30% transmission, a shoulder peak starts to form at the low-q side of the α-iron (110) peak, indicating an XFEL-induced thermal expansion. At 50% transmission, this shoulder peak grows and shifts further toward the low-q side, and above 70% transmission, high-temperature fcc-Fe (γ-iron) is observed by the appearance of its (111) peak. The transformation of α- to γ-iron would require at least 900 K at 5 GPa.[33] Given the refined peak positions and the established EOS of the iron phases,[34] we estimate residual temperatures of 750 and 1270 K at 50 and 70% fluence (2400 and 3900 K calculated peak temperatures), respectively (Figure 3a). The reaction between Fe and N_2, however, did not occur even at the full 100% transmission in run A, at which point the residual temperature is estimated to be 1424 K (5700 K peak temperature). The ~70% cooling between the pump and the probe is consistent with expectations for Fe samples.[29] The pulse-to-pulse energy variance of the XFEL, of order 30%, could lead to differing heating in shorter duration experiments, whereas in longer duration studies, where reactions products appear, only the averaged heating and duration is important. Thus, temperatures measured following single pulses (pump−probe) are consistent with expected values including initial volumetric X-ray absorption and heat transfer between pulses;[29] somewhat higher temperatures are expected after serial exposures in a MHz pulse train, because of heat accumulation;[29] thus, the temperature conditions reported following single pulses are lower bounds on those achieved after second and subsequent pulses in a train.

In contrast, XFEL-induced chemical reaction between Fe and N_2 is observed in the runs B and C (Figure 3a). The new peaks observed both *in situ* and *ex situ* after exposure during run B are indexed as an ε-Fe_3N_{1+x} phase (Figure 3b). When we exposed the sample with serial XFEL trains for 11 s (run C), the formation of the ε-Fe_3N_{1+x} was observed from the third train by the growth of its (002) and (111) peaks (Figure 3c). In the first and second trains, we observed the growth of (111) and (002) Bragg reflections of fcc-Fe indicating temperatures of 1490 and 1680 K, respectively. From the third train where ε-Fe_3N_{1+x} formed, the temperature was maintained between 1340 and 1780 K up to the 14th train where the Bragg peaks of fcc-Fe disappeared. The ε-Fe_3N_{1+x} (and residual bcc-Fe) remained until the last train without any systematic changes in the relative peak intensities and positions. We estimate a cumulative absorbed energy of 3 mJ for the chemical reaction of Fe and N_2 at the precompression conditions of 5 GPa.

The sample pressure after run C increased to 7.8(1) GPa, where the unit cell parameters of ε-Fe_3N_{1+x} are refined to a = 4.707(1) Å and c = 4.357(1) Å in the space group $P6_322$ (no. 182) (Figure 3d). It is well-established that the unit-cell volume of ε-Fe_3N_{1+x} is linearly proportional to the increasing nitrogen content x at ambient pressure.[35,36] The refined unit cell volume

https://doi.org/10.1021/acs.jpclett.1c00150
J. Phys. Chem. Lett. 2021, 12, 3246−3252

of the recovered ε-Fe_3N_{1+x}, e.g., 83.59(3) Å^3 at 7.8(1) GPa, would correspond to ε-Fe_3N_{1+x} with x = 0.33 at ambient conditions, assuming an EOS of B_0 = 172 GPa and B' = 5.7 as derived previously.[35−37] We therefore conclude that the composition of the XFEL-induced synthesis product is $Fe_3N_{1.33}$.

To investigate the cross-sectional textures and chemical distribution of the $Fe_3N_{1.33}$ reaction product, we have prepared the sample from run B using a focused Ga ion beam (FIB, 30 kV and 10 pA to 30 nA for surfacing) and performed scanning electron microscopy (SEM) (ZEISS Crossbeam 540 at Yonsei University) and scanning transmission electron microscope imaging (STEM, JEOL JEM-F200 combined with energy-dispersive X-ray spectroscopy) (Figure 4). The sample was mounted on a Cu grid and measured in the annular dark-field mode. A two-dimensional elemental distribution of the cross-sectioned sample shown in Figure 4c,d reveals that over the 4 μm thickness of the original Fe-foil, the distribution of Fe and N appears to be uniform with regularly spaced holes representing degassed N_2 after the recovery of the sample. STEM data corroborate the results of the *in situ* and *ex situ* XRD by showing the distribution of the ABAB type stacking and distance between the Fe atoms, as expected for the ε-Fe_3N_{1+x} structure (Figure 4b). It is remarkable that such a homogeneous composition is obtained after such a short cumulative heating time as atomic nitrogen diffusion is in general a much slower process.[38]

In conclusion, our work demonstrates that the required activation energy for chemical reactions controlled by the XFEL radiation is an important experimental parameter. Despite only a limited number of exposures due to constraints and availability of *in* and *ex situ* characterizations, we are confident that the XFEL parameters of our studies are well within parameters that are reproducible and in agreement with the known behavior of the Fe−N_2 system under high pressure and temperature. In contrast, the kinetics of the XFEL-induced synthesis of ε-$Fe_3N_{1.33}$ are noteworthy and unprecedented. We found a remarkably homogeneous reaction product after the ultrafast reaction between Fe and nitrogen in a DAC at pressures above 5 GPa and temperatures exceeding 1400 K as pumped and probed by consecutive XFEL pulses separated by 443 ns. Following chemical reactions between gas and solid at high pressures and temperatures in a DAC using a tailored pump−probe setup at an XFEL opens up a new parameter space for the exploration of new materials forming on fast time scales at high pressure.

AUTHOR INFORMATION

Corresponding Authors

R. Stewart McWilliams − *The School of Physics and Astronomy, Centre for Science at Extreme Conditions and SUPA, University of Edinburgh, Edinburgh EH9 3FD, U.K.;* orcid.org/0000-0002-3730-8661; Email: rs.mcwilliams@ed.ac.uk

Yongjae Lee − *Earth System Sciences, Yonsei University, Seoul 03722, Republic of Korea;* orcid.org/0000-0002-2043-0804; Email: yongjaelee@yonsei.ac.kr

Authors

Huijeong Hwang − *Earth System Sciences, Yonsei University, Seoul 03722, Republic of Korea*

Taehyun Kim − *Earth System Sciences, Yonsei University, Seoul 03722, Republic of Korea*

Hyunchae Cynn − *Lawrence Livermore National Laboratory, Livermore, California 94550, United States*

Thomas Vogt − *Nano Center and Department of Chemistry and Biochemistry, University of South Carolina, Columbia, South Carolina 29208, United States;* orcid.org/0000-0002-4731-2787

Rachel J. Husband − *Photon Sciences, Deutsches Elektronen-Synchrotron (DESY), Hamburg 22607, Germany*

Karen Appel − *European XFEL GmbH, 22869 Schenefeld, Germany*

Carsten Baehtz − *Institute of Radiation Physics, Helmholtz-Zentrum Dresden-Rossendorf, 01328 Dresden, Germany*

Orianna B. Ball − *The School of Physics and Astronomy, Centre for Science at Extreme Conditions and SUPA, University of Edinburgh, Edinburgh EH9 3FD, U.K.*

Marzena A. Baron − *Inst. Minéralogie, de Physique des Matériaux et de Cosmochimie (IMPMC), Sorbonne University, Paris, France*

Richard Briggs − *Lawrence Livermore National Laboratory, Livermore, California 94550, United States*

Maxim Bykov − *Carnegie Science, Earth and Planets Laboratory, Washington, D.C. 20015, United States;* orcid.org/0000-0003-0248-1728

Elena Bykova − *Carnegie Science, Earth and Planets Laboratory, Washington, D.C. 20015, United States*

Valerio Cerantola − *European XFEL GmbH, 22869 Schenefeld, Germany*

Julien Chantel − *Univ. Lille, F-59000 Lille, France*

Amy L. Coleman − *Lawrence Livermore National Laboratory, Livermore, California 94550, United States*

Dana Dattlebaum − *Los Alamos National Laboratory, Los Alamos, New Mexico 87545, United States*

Leora E. Dresselhaus-Marais − *Lawrence Livermore National Laboratory, Livermore, California 94550, United States;* orcid.org/0000-0002-0757-0159

Jon H. Eggert − *Lawrence Livermore National Laboratory, Livermore, California 94550, United States*

Lars Ehm − *Mineral Physics Institute, Stony Brook University, Stony Brook, New York 11794, United States*

William J. Evans − *Lawrence Livermore National Laboratory, Livermore, California 94550, United States*

Guillaume Fiquet − *Inst. Minéralogie, de Physique des Matériaux et de Cosmochimie (IMPMC), Sorbonne University, Paris, France*

Mungo Frost − *SLAC National Accelerator Laboratory, Menlo Park, California 94025, United States*

Konstantin Glazyrin − *Photon Sciences, Deutsches Elektronen-Synchrotron (DESY), Hamburg 22607, Germany*

Alexander F. Goncharov − *Carnegie Science, Earth and Planets Laboratory, Washington, D.C. 20015, United States;* orcid.org/0000-0002-6422-8819

Zsolt Jenei − *Lawrence Livermore National Laboratory, Livermore, California 94550, United States*

Jaeyong Kim − *Department of Physics, Research Institute for Natural Science, HYU-HPSTAR-CIS High Pressure Research Center, Hanyang University, Seoul 04763, Republic of Korea;* orcid.org/0000-0003-1787-3775

Zuzana Konôpková − *European XFEL GmbH, 22869 Schenefeld, Germany*

Jona Mainberger − *Photon Sciences, Deutsches Elektronen-Synchrotron (DESY), Hamburg 22607, Germany*

Mikako Makita − *European XFEL GmbH, 22869 Schenefeld, Germany*

Hauke Marquardt − *Department of Earth Sciences, University of Oxford, OX1 3AN Oxford, United Kingdom*

https://doi.org/10.1021/acs.jpclett.1c00150
J. Phys. Chem. Lett. 2021, 12, 3246−3252

Emma E. McBride − *SLAC National Accelerator Laboratory, Menlo Park, California 94025, United States*
James D. McHardy − *The School of Physics and Astronomy, Centre for Science at Extreme Conditions and SUPA, University of Edinburgh, Edinburgh EH9 3FD, U.K.*
Sébastien Merkel − *Univ. Lille, F-59000 Lille, France*
Guillaume Morard − *Inst. Minéralogie, de Physique des Matériaux et de Cosmochimie (IMPMC), Sorbonne University, Paris, France; Université Grenoble Alpes, 38000 Grenoble, France*
Earl F. O'Bannon, III − *Lawrence Livermore National Laboratory, Livermore, California 94550, United States*
Christoph Otzen − *Photon Sciences, Deutsches Elektronen-Synchrotron (DESY), Hamburg 22607, Germany*
Edward J. Pace − *The School of Physics and Astronomy, Centre for Science at Extreme Conditions and SUPA, University of Edinburgh, Edinburgh EH9 3FD, U.K.*
Alexander Pelka − *Institute of Radiation Physics, Helmholtz-Zentrum Dresden-Rossendorf, 01328 Dresden, Germany*
Charles M. Pépin − *CEA, F-91297 Arpajon, France; Université Paris-Saclay, Laboratoire Matière en Conditions Extrêmes, 91680 Bruyères-le-Châtel, France*
Jeffrey S. Pigott − *Los Alamos National Laboratory, Los Alamos, New Mexico 87545, United States; Case Western Reserve University, Cleveland, Ohio 44106, United States*
Vitali B. Prakapenka − *Center for Advanced Radiation Sources, University of Chicago, Chicago, Illinois 60637, United States*
Clemens Prescher − *Photon Sciences, Deutsches Elektronen-Synchrotron (DESY), Hamburg 22607, Germany*
Ronald Redmer − *Institut für Physik, Universität Rostock, D-18051 Rostock, Germany*
Sergio Speziale − *GFZ German Research Centre for Geosciences, 14473 Potsdam, Germany*
Georg Spiekermann − *Institut für Geowissenschaften, Universität Potsdam, 14476 Potsdam, Germany*
Cornelius Strohm − *Photon Sciences, Deutsches Elektronen-Synchrotron (DESY), Hamburg 22607, Germany*
Blake T. Sturtevant − *Los Alamos National Laboratory, Los Alamos, New Mexico 87545, United States*
Nenad Velisavljevic − *Lawrence Livermore National Laboratory, Livermore, California 94550, United States*
Max Wilke − *Institut für Geowissenschaften, Universität Potsdam, 14476 Potsdam, Germany*
Choong-Shik Yoo − *Department of Chemistry, Institute of Shock Physics, and Materials Science and Engineering, Washington State University, Pullman, Washington 99164, United States;* orcid.org/0000-0002-2664-0730
Ulf Zastrau − *European XFEL GmbH, 22869 Schenefeld, Germany*
Hanns-Peter Liermann − *Photon Sciences, Deutsches Elektronen-Synchrotron (DESY), Hamburg 22607, Germany*
Malcolm I. McMahon − *The School of Physics and Astronomy, Centre for Science at Extreme Conditions and SUPA, University of Edinburgh, Edinburgh EH9 3FD, U.K.*

Complete contact information is available at: https://pubs.acs.org/10.1021/acs.jpclett.1c00150

Notes

The authors declare no competing financial interest.

■ ACKNOWLEDGMENTS

We thank H. Sinn for experimental assistance and T. Tschentscher and S. Pascarelli for fruitful discussions. This work was supported by the Leader Researcher program (NRF-2018R1A3B1052042) of the Korean Ministry of Science, ICT and Planning (MSIP). We also thank the supports by NRF-2019K1A3A7A09033395 and NRF-NRF-2016K1A4A3914691 grants of the MSIP. We acknowledge European XFEL in Schenefeld, Germany, for provision of X-ray free-electron laser beamtime at Scientific Instrument HED (High Energy Density Science) and thank the staff for their assistance. The authors are indebted to the Helmholtz International Beamline for Extreme Fields (HIBEF) user consortium for the provision of instrumentation and staff that enabled this experiment. We acknowledge DESY (Hamburg, Germany), a member of the Helmholtz Association HGF, for the provision of experimental facilities. Parts of this research were carried out at PETRA III (beamline P02.2). The research leading to this result has been supported by the project CALIPSOplus under the Grant Agreement 730872 from the EU Framework Program for Research and Innovation HORIZON 2020. Part of this work was performed under the auspices of the U.S. Department of Energy by Lawrence Livermore National Laboratory under Contract No. DE-AC52-07NA27344 and by the US Department of Energy through the Los Alamos National Laboratory, operated by Triad National Security, LLC, for the National Nuclear Security Administration (Contract No. 89233218CNA000001). Research presented in this Letter was supported by the Department of Energy, Laboratory Directed Research and Development program at Los Alamos National Laboratory under Project Number 20190643DR and at SLAC National Accelerator Laboratory, under contract DE-AC02-76SF00515. Support is acknowledged from the Panofsky Fellowship at SLAC (awarded to EEM); the DOE Office of Fusion Energy Science funding number FWP100182 (MF and EEM); EPSRC Grants EP/P024513/1 (RSM) and EP/R02927X/1 (E.J.P. and M.I.M.); the European Research Council (ERC) under the European Union's Horizon 2020 research and innovation Programme for Grant Agreement Nos. 670787 (G.F., M.A.B., and G.M.) and 864877 (H.M.). K.A., K.G., R.H., Z.K., H.P.L., and R.R. thank the DFG for support within the Research Unit FOR 2440. S.M. and J.C. acknowledge support from the I-SITE ULNE project MetalCore (R-ERCGEN-19-006-MERKEL). C.S.Y. acknowledges DOE-NNSA (DE-NA0003342), NSF (DMR-1701360), and ARO (W911NF-17-1-0468).

■ REFERENCES

(1) Dawes, A.; Mason, N. J.; Tegeder, P.; Holtom, P. Laboratory Synthesis of Astrophysical Molecules. In *Electron Scattering From Atoms, Molecules*; Whelan, C. T., Mason, N. J., Eds.; Springer: Boston, MA, 2005; pp 329−340.
(2) Adler, J. F.; Willams, Q. A high-pressure X-ray diffraction study of iron nitrides: Implications for Earth's core. *J. Geophys. Res.* **2005**, *110*, B01203.
(3) Labidi, J.; Barry, P. H.; Bekaert, D. V.; Broadley, M. W.; Marty, B.; Giunta, T.; Warr, O.; Sherwood Lollar, B.; Fischer, T. P.; Avice, G.; Caracausi, A.; Ballentine, C. J.; Halldórsson, S. A.; Stefánsson, A.; Kurz, M. D.; Kohl, I. E.; Young, E. D. Hydrothermal $^{15}N^{15}N$ abundances constrain the origins of mantle nitrogen. *Nature* **2020**, *580*, 367−371.
(4) Mikhail, S.; Sverjensky, D. A. Nitrogen speciation in upper mantle fluids and the origin of Earth's nitrogen-rich atmosphere. *Nat. Geosci.* **2014**, *7*, 816−819.

(5) Miao, M.; Wang, X.; Brgoch, J.; Spera, F.; Jackson, M. G.; Kresse, G.; Lin, H. Anionic Chemistry of Noble Gases: Formation of Mg-NG (NG = Xe, Kr, Ar) Compounds under Pressure. *J. Am. Chem. Soc.* **2015**, *137*, 14122−14128.
(6) Zhu, L.; Liu, H.; Pickard, C. J.; Zou, G.; Ma, Y. Reactions of xenon with iron and nickel are predicted in the Earth's inner core. *Nat. Chem.* **2014**, *6*, 644−648.
(7) Zaleski-Ejgierd, P.; Lata, P. M. Krypton oxides under pressure. *Sci. Rep.* **2016**, *6*, 18938.
(8) Liu, Z.; Botana, J.; Hermann, A.; Valdez, S.; Zurek, E.; Yan, D.; Lin, H.; Miao, M. Reactivity of He with ionic compounds under high pressure. *Nat. Commun.* **2018**, *9*, 951.
(9) Adeleke, A. A.; Kunz, M.; Greenberg, E.; Prakapenka, V. B.; Yao, Y.; Stavrou, E. A High-Pressure Compound of Argon and Nickel: Noble Gas in the Earth's Core? *ACS Earth Space Chem.* **2019**, *3*, 2517−2524.
(10) Crépisson, C.; Sanloup, C.; Blanchard, M.; Hudspeth, J.; Glazyrin, K.; Capitani, F. The Xe-SiO_2 System at Moderate Pressure and High Temperature. *Geochem., Geophys., Geosyst.* **2019**, *20*, 992−1003.
(11) Rahm, M.; Cammi, R.; Ashcroft, N. W.; Hoffmann, R. Squeezing All Elements in the Periodic Table: Electron Configuration and Electronegativity of the Atoms under Compression. *J. Am. Chem. Soc.* **2019**, *141*, 10253−10271.
(12) Mao, H.-K.; Chen, B.; Chen, J.; Li, K.; Lin, J.-F.; Yang, W.; Zheng, H. Recent advances in high-pressure science and technology. *Matter Radiat. Extrem.* **2016**, *1*, 59−75.
(13) Pace, E. J.; Coleman, A. L.; Husband, R. J.; Hwang, H.; Choi, J.; Kim, T.; Hwang, G.; Chun, S. H.; Nam, D.; Kim, S.; Ball, O. B.; Liermann, H.-P.; McMahon, M. I.; Lee, Y.; McWilliams, R. S. Intense Reactivity in Sulfur-Hydrogen Mixtures at High Pressure under X-ray Irradiation. *J. Phys. Chem. Lett.* **2020**, *11* (5), 1828−1834.
(14) Adler, J. F.; Williams, Q. A high-pressure X-ray diffraction study of iron nitrides: Implications for Earth's core. *J. Geophys. Res.* **2005**, *110*, B011203.
(15) Zhang, Y.; Wang, Q. Magnetic-Plasmonic Dual Modulated FePt-Au Ternary Heterostructured Nanorods as a Promising Nano-Bioprobe. *Adv. Mater.* **2012**, *24*, 2485−2490.
(16) Mahmoudi, M.; Shokrgozar, M. A. Multifunctional stable fluorescent magnetic nanoparticles. *Chem. Commun.* **2012**, *48*, 3957−3959.
(17) Arabczyk, W.; Pelka, R. Studies of the Kinetics of Two Parallel Reactions: Ammonia Decomposition and Nitriding of Iron Catalyst. *J. Phys. Chem. A* **2009**, *113*, 411−416.
(18) Hasegawa, M.; Yagi, T. Systematic study of formation and crystal structure of 3d-transition metal nitrides synthesized in a supercritical nitrogen fluid under 10 GPa and 1800 K using diamond anvil cell and YAG laser heating. *J. Alloys Compd.* **2005**, *403*, 131−142.
(19) Clark, W. P.; Steinberg, S.; Dronskowski, R.; McCammon, C.; Kupenko, I.; Bykov, M.; Dubrovinsky, L.; Akselrud, L. G.; Schwarz, U.; Niewa, R. High-Pressure NiAs-Type Modification of FeN. *Angew. Chem., Int. Ed.* **2017**, *56*, 7302−7306.
(20) Bykov, M.; Bykova, E.; Aprilis, G.; Glazyrin, K.; Koemets, E.; Chuvashova, I.; Kupenko, I.; McCammon, C.; Mezouar, M.; Prakapenka, V.; Liermann, H.-P.; Tasnádi, F.; Ponomareva, A. V.; Abrikosov, I. A.; Dubrovinskaia, N.; Dubrovinsky, L. Fe-N system at high pressure reveals a compound featuring polymeric nitrogen chains. *Nat. Commun.* **2018**, *9*, 2756.
(21) Bykov, M.; Khandarkhaeva, S.; Fedotenko, T.; Sedmak, P.; Dubrovinskaia, N.; Dubrovinsky, L. Synthesis of FeN_4 at 180 GPa and its crystal structure from a submicron-sized grain. *Acta Crystallogr.* **2018**, *E74*, 1392−1395.
(22) Laniel, D.; Dewaele, A.; Anzellini, S.; Guignot, N. Study of the iron nitride FeN into the megabar regime. *J. Alloy. Compd.* **2018**, *733*, 53−58.
(23) Laniel, D.; Dewaele, A.; Garbarino, G. High Pressure and High Temperature Synthesis of the Iron Pernitride FeN_2. *Inorg. Chem.* **2018**, *57*, 6245−6251.
(24) Leineweber, A.; Jacobs, H.; Huning, F.; Lueken, H.; Schilder, H.; Kockelmann, W. ϵ-Fe_3N: magnetic structure, magnetization, and temperature dependent disorder of nitrogen. *J. Alloys Compd.* **1999**, *288*, 79−87.
(25) Mcwilliams, R. S. *Femtosecond Hard X-ray Studies at High Static Pressure*; 2019, 002292. .
(26) Decking, W.; et al. A MHz-repetition-rate hard X-ray free-electron laser driven by a superconducting linear accelerator. *Nat. Photonics* **2020**, *14*, 391−397.
(27) Grünert, J.; Carbonell, M. P.; Dietrich, F.; Falk, T.; Freund, W.; Koch, A.; Kujala, N.; Laksman, J.; Liu, J.; Maltezopoulos, T.; Tiedtke, K.; Jastrow, U. F.; Sorokin, A.; Syresin, E.; Grebentsov, A.; Brovko, O. X-ray photon diagnostics at the European XFEL. *J. Synchrotron Radiat.* **2019**, *26*, 1422−1431.
(28) Maltezopoulos, T.; Dietrich, F.; Freund, W.; Jastrow, U. F.; Koch, A.; Laksman, J.; Liu, J.; Planas, M.; Sorokin, A. A.; Tiedtke, K.; Grünert, J. Operation of X-ray gas monitors at the European XFEL. *J. Synchrotron Radiat.* **2019**, *26*, 1045−1051.
(29) Meza-Galvez, J.; Gomez-Perez, N.; Marshall, A. S.; Coleman, A. L.; Appel, K.; Liermann, H. P.; McMahon, M. I.; Konôpková, Z.; McWilliams, R. S. Thermomechanical response of thickly tamped targets and diamond anvil cells under pulsed hard X-ray irradiation. *J. Appl. Phys.* **2020**, *127*, 195902.
(30) Mao, H. K.; Xu, J.; Bell, P. M. Calibration of the Ruby Pressure Gauge to 800 kbar Under Quasi-Hydrostatic Conditions. *J. Geophys. Res.* **1986**, *91*, 4673−4676.
(31) Dewaele, A.; Torrent, M.; Loubeyre, P.; Mezouar, M. Compression curves of transition metals in the Mbar range: Experiments and projector augmented-wave calculations. *Phys. Rev. B: Condens. Matter Mater. Phys.* **2008**, *78*, 104102.
(32) Prescher, C.; Prakapenka, V. B. DIOPTAS: a program for reduction of two-dimensional X-ray diffraction data and data exploration. *High Pressure Res.* **2015**, *35* (3), 223−230.
(33) Dewale, A.; Svitlyk, V.; Bottin, F.; Bouchet, J.; Jacobs, J. Iron under conditions close to the $\alpha-\gamma-\epsilon$ triple point. *Appl. Phys. Lett.* **2018**, *112*, 201906.
(34) Dorogokupets, P. I.; Dymshits, A. M.; Litasov, K. D.; Sokolova, T. S. Thermodynamics and Equations of State of Iron to 350 GPa and 6000 K. *Sci. Rep.* **2017**, *7*, 41863.
(35) Guo, K.; Rau, D.; von Appen, J.; Prots, Y.; Schnelle, W.; Dronskowski, R.; Niewa, R.; Schwarz, U. High pressure high-temperature behavior and magnetic properties of Fe_4N: experiment and theory. *High Pressure Res.* **2013**, *33* (3), 684−696.
(36) Leineweber, A.; Jacobs, H.; Hüning, F.; Lueken, H.; Kockelmann, W. Nitrogen ordering and ferromagnetic properties of ϵ-Fe_3N_{1+x} ($0.10 \leq x \leq 0.39$) and ϵ-$Fe_3(N_{0.80}C_{0.20})_{1.38}$. *J. Alloys Compd.* **2001**, *316*, 21−38.
(37) Niewa, R.; Rau, D.; Wosylus, A.; Meier, K.; Hanfland, M.; Wessel, M.; Dronskowski, R.; Dzivenko, D. A.; Riedel, R.; Schwarz, U. High-Pressure, High-Temperature Single-Crystal Growth, Ab initio Electronic Structure Calculations, and Equation of State of ϵ-Fe_3N_{1+x}. *Chem. Mater.* **2009**, *21*, 392−398.
(38) Glasson, D. R.; Jayaweera, S. A. A. Formation and Reactivity of Nitrides. I. Review and Introduction. *J. Electrochem. Soc.* **1954**, *1010*, 171−175.

https://doi.org/10.1021/acs.jpclett.1c00150
J. Phys. Chem. Lett. 2021, 12, 3246−3252